Chemical Physics 404 (2012) 64–73

Contents lists available at SciVerse ScienceDirect

Chemical Physics

journal homepage: www.elsevier.com/locate/chemphys

Quantum chemical studies of photochromic properties of benzoxazine compound

Stepas Toliautas [a,*], Juozas Sulskus [a], Leonas Valkunas [a,b], Mikas Vengris [c]

[a] Department of Theoretical Physics, Vilnius University, Saulėtekio 9-III, LT-10222 Vilnius, Lithuania
[b] Institute of Physics, Center for Physical Sciences and Technology, Savanorių 231, LT-02300 Vilnius, Lithuania
[c] Department of Quantum Electronics, Vilnius University, Saulėtekio 9-III, LT-10222 Vilnius, Lithuania

ARTICLE INFO

Article history:
Available online 16 March 2012

Keywords:
Photochromism
Electronic excited states
Potential energy surfaces
Quantum chemical computations

ABSTRACT

Molecular electronic structure of ground and excited states of a photochromic indolo[2,1-*b*][1,3]benzoxazine compound incorporating closed-ring system, which opens upon UV light excitation, was studied using various quantum chemical methods. Three local minima of the ground electronic state potential energy surface and related transition states were identified along the path of rotation of 4-nitrophenol group. Additionally, three local minima of the excited electronic states were located. The evaluated transition energy barriers between local ground-state minima nearest to the initial structure of the investigated molecule are less than 2 k_BT, making open structures likely to revert to the initial structure by thermalization. Results obtained using *ab initio* GMC–QDPT method were explored and compared to the widely used TD-DFT and semi-empiric ZINDO methods.

1. Introduction

Photochromic compounds are light-sensitive molecular systems which exhibit changes of absorption properties during photo-induced processes. Changes in the absorption spectrum indicate energy transfer and structural transformations of the system [1], which are reversible by thermal dissipation or by photoexcitation of a different wavelength in most cases. Possible applications of such compounds include molecular-scale electronics and high density data storage [2]. Among the various compounds, spiropyrans are remarkable for their ability to undergo reversible ring opening upon photoexcitation [3,4]. The cycle can be repeated many times without appreciable degradation of the system [5]. This opens a possibility to study excitation dynamics of a photochromic system both theoretically and experimentally, using ultrafast spectroscopy [6] instead of or in conjunction with IR or NMR spectra [7]. Another similar photoactive materials used to study photochromism are coumarins (references in [8] for experiments and [9] for theoretical research) and ruthenium polypyridine complexes (references in [10]).

The compound that is studied here, 5a,6-dihydro-12h-indolo[2,1-*b*][1,3]benzoxazine, belongs to a group of recently synthesized indolo-benzoxazines [5,11], which upon excitation exhibit fast C–O bond cleavage and formation of two distinct chromophoric groups. It has been stated recently that absorption spectra of the IB compound (Fig. 1) in its opened and closed ring configurations can be sufficiently well understood as a combination of spectral features characteristic to its constituent moieties [5,12]. According to the experimental observations, the ground-state absorption spectrum of the IB compound peaks around 300 nm [6,12], and the crystal structure indicates that the indole and oxazine ring planes are nearly perpendicular to each other [5]. When the compound is treated with organic base, a strong absorption band appears in the visible range (around 430 nm) matching closely the absorption of isolated 4-nitrophenolate [6,12]. When the oxygen on 4-nitrophenolate is protonated, the absorption peak shifts to the blue (maximum is now at 310 nm) and twofold decrease in the extinction coefficient is observed [6]. Femtosecond dynamics of the IB photochromic switch is extremely complex. To some degree it is possible to interpret it as a combination of the dynamics observed in the 3H-indolium and 4-nitrophenolate compounds [6]. However, many questions remain unanswered; some of them are a target of this theoretical investigation. One important aspect is the number of excited states comprising the lowest ground-state absorption band, and their interplay in the photo-induced dynamics. Additionally, if these states are localized on a certain part of the molecular backbone, it is important to know which part it is, in order to be able to intelligently synthesize new compounds with desired properties.

Theoretical modeling of the molecular systems using methods derived from first principles (*ab initio*) is generally regarded as the most accurate way for treating such systems. However, due to computational difficulties, many *ab initio* methods are still limited to the studies of small or well understood molecules. Popular approaches for more complex systems include time-dependent

* Corresponding author. Address: Faculty of Physics, Vilnius University, Saulėtekio 9-III, LT-10222 Vilnius, Lithuania. Tel.: +370 5 2366049; fax: +370 5 2366003.
E-mail addresses: stepas.toliautas@ff.stud.vu.lt (S. Toliautas), juozas.sulskus@ff.vu.lt (J. Sulskus), leonas.valkunas@ff.vu.lt (L. Valkunas), mikas.vengris@ff.vu.lt (M. Vengris).

0301-0104/$ - see front matter © 2012 Elsevier B.V. All rights reserved.
http://dx.doi.org/10.1016/j.chemphys.2012.03.006

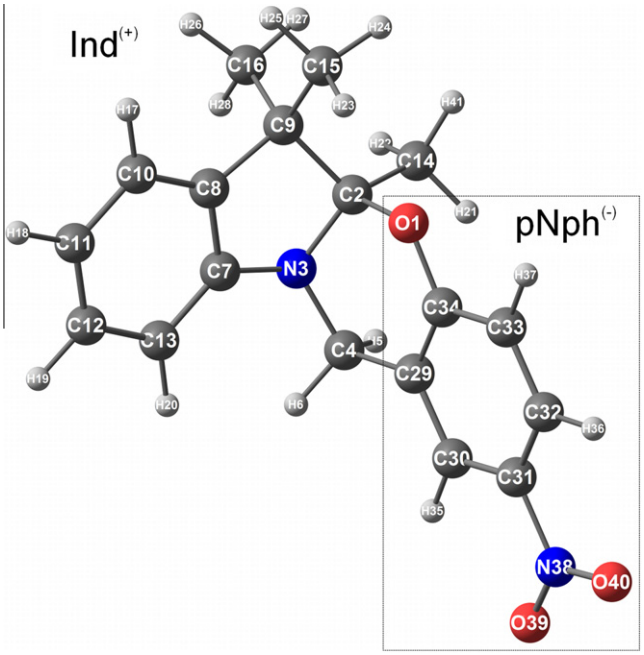

Fig. 1. Structure and numbering of atoms in 5a,6-dihydro-12h-indolo[2,1-*b*][1,3]benzoxazine (IB) compound.

density-functional theory (TD-DFT) [13–16] with hybrid functionals and semi-empiric ZINDO method [17,18]. These methods provide excitation energy values that are comparable to experimental data. On the other hand, use of empirical parameters for such methods and the fact that they are based on the account of only singly excited configurations may cause inaccuracy during evaluation of potential energy surfaces of deformed molecules. The application of more sophisticated configuration-interaction based (CI) and multiconfigurational (MC) methods accounting for configurations with higher degree of excitation may answer a question about the character of wavefunctions of the excited states and support the findings of the TD-DFT and ZINDO. Most of *ab initio* methods used so far in practice give inaccurate excitation energy values. One of the advanced methods that seems to avoid this drawback is the multiconfigurational quasidegenerate perturbation theory (MC-QDPT) using general multiconfiguration (GMC) SCF wave functions as reference functions (GMC–QDPT) [19–21]. In a recent study of the excited states of 7-aminocoumarines [9] GMC–QDPT showed a better performance than the standard MC-QDPT with smaller active space and yielded excitation energy values close to the experiment. To assess the relevance of this method for compound under investigation, properties calculated using GMC–QDPT are compared to the results of calculations using the TD-DFT and ZINDO methods.

Another issue concerning studies of photochromic compounds by means of the TD-DFT method is the underestimation of Rydberg excitation energies, oscillator strengths, and charge-transfer excitation energies. It is presumed that poor TD-DFT results for pure functionals may be due to their lack of a long-range orbital–orbital interaction. To overcome that, the long-range correction (LC) scheme for exchange functionals of the density functional theory to TD-DFT [22] is applied during the excited-state calculations. This scheme was shown to give results comparable to the ones obtained by the CI-based CAS-PT2 method by investigating small twisted intramolecular charge transfer (TICT) systems [23]. For the optimized geometry of the charge transfer state of 4-(1-pyrrolyl)-pyridine (PP) molecule, CAS-PT2 gave a lower total charge transfer state energy for the LC-TDDFT optimized geometry than the energy obtained for other geometries. LC-TDDFT also provided close energies to those of CAS-PT2 for both the absorption and fluorescence, as well as nonzero oscillator strength for the fluorescence.

Here we present a theoretical quantum-chemical study of the IB compound and its chromophoric groups. Our calculations focus on singlet excited states only because experimental studies have shown no singlet oxygen production upon excitation of IB-type molecules under aerobic conditions [5]. Therefore it is assumed that triplet excited states are not a significant factor in the photo-induced dynamics of IB. Using methods described above, we consider and analyze potential energy surfaces and features of the electronic spectrum along possible reaction coordinates of photoisomerization of the IB molecule. The purpose of the investigation is to evaluate the possible ways of "on–off" switching of photochromic compound by comparison of theoretical features of electronic excited states with the results of absorption studies from ultrafast responses of the IB molecule and its model compounds [6].

2. Computational details

Molecular ground-state structures of the 5a,6-dihydro-12h-indole[2,1-b][1,3]benzoxazine (IB) compound and its molecular groups, 4-nitrophenol (neutral pNph and ionized $pNphe^{-}$ forms) and 1,2,3,3-tetramethyl-3H-indolium (Ind^{+}) (Fig. 1), were obtained by optimizing their geometric parameters. The ground-state optimizations were performed using electronic structure modeling suite *Gaussian03* [24]. The DFT method [25–27] with hybrid B3LYP functional [28–30] and 6-311++(2d,p) basis set [31–34] was used for the optimization. In addition to the structure of the global minimum on the ground-state energy surface of the IB compound – denoted M0 further on – three structures corresponding to the local minima of the ground-state potential energy surface (PES) were located by performing optimization from various starting configurations. These local minima are hereafter referred to as M1, M2 and M3. Structure corresponding to M1 is obtained from M0 structure by rotating the pNph group counterclockwise around the C_4–C_{29} bond (Fig. 1). Structures M2 and M3 may be obtained as the result of rotation in the opposite direction. Local minimum M3 is represented by a structure with almost reversed pNph group position compared to the M0 structure. Transition state structures between the global minimum structure M0 and structures M1 and M2 were found by subsequent calculations using synchronous transit-guided quasi-Newton (STQN) method, as implemented in *Gaussian03* [35,36]. Notations T01 and T02 in the text correspond

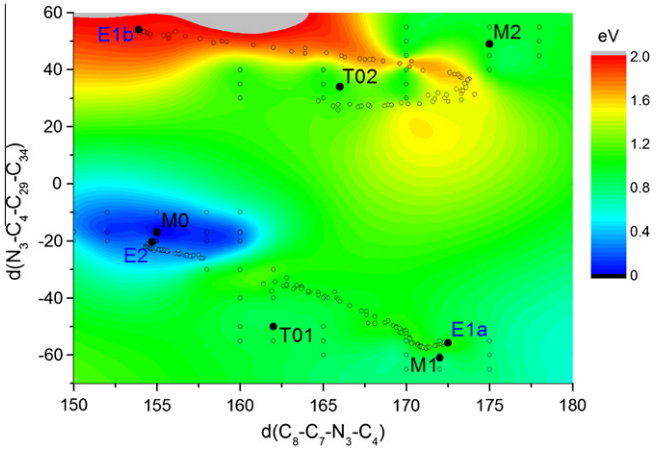

Fig. 2. The ground-state potential energy surface of the IB compound as a function of two dihedral angles (see Table 2). Labels denote main stationary points on the surface (explained in the text). Open circles mark actual data points.

Table 1a
Structural parameters of the model compounds of the IB molecule (calculated using DFT B3LYP functional with 6-311++(2d,p) basis set). *Columns:* pNph – neutral 4-nitrophenol; $pNphe^-$ – 4-nitrophenol ion; Ind^+ – 3H-indolium ion.

Bond lengths (Å)					Valence angles (deg)				
Bond	Ind^+	Bond	pNph	$pNphe^-$	Angle	Ind^+	Angle	pNph	$pNphe^-$
$C_{13}–C_{12}$	1.393	$C_{34}–O_1$	1.358	1.253	$C_{13}–C_{12}–C_{11}$	120.96	$C_2–O_1–C_{34}$	110.32[a]	
$C_{12}–C_{11}$	1.395	$C_{34}–C_{33}$	1.397	1.453	$C_{11}–C_{10}–C_8$	118.38	$O_1–C_{34}–C_{33}$	117.14	122.67
$C_{11}–C_{10}$	1.396	$C_{33}–C_{32}$	1.382	1.367	$C_8–C_7–C_{13}$	123.82	$C_{29}–C_{34}–C_{33}$	120.34	114.66
$C_{10}–C_8$	1.384	$C_{32}–C_{31}$	1.392	1.412	$C_{10}–C_8–C_9$	131.93	$C_{33}–C_{32}–C_{31}$	119.38	120.62
$C_8–C_7$	1.389	$C_{31}–C_{30}$	1.389	1.412	$C_{13}–C_7–N_3$	128.23	$C_{31}–C_{30}–C_{29}$	119.20	120.62
$C_7–C_{13}$	1.384	$C_{30}–C_{29}$	1.385	1.367	$C_9–C_2–N_3$	110.67	$C_{32}–C_{31}–N_{38}$	119.38	120.40
$C_8–C_9$	1.513	$C_{29}–C_{34}$	1.397	1.453	$C_8–C_9–(C_{16})H_3$	112.32	$C_{31}–N_{38}–O_{40}$	117.79	119.31
$C_9–C_2$	1.514	$C_{31}–N_{38}$	1.465	1.409	$C_8–C_9–(C_{15})H_3$	112.32	$O_{39}–N_{38}–O_{40}$	124.40	121.37
$C_2–N_3$	1.304	$N_{38}–O_{39}$	1.227	1.252	$C_9–C_2–(C_{14})H_3$	125.19			
$C_7–N_3$	1.434	$N_{38}–O_{40}$	1.227	1.252	$C_7–N_3–(C_4)H_3$	121.71			
$C_9–(C_{16})H_3$	1.549								
$C_9–(C_{15})H_3$	1.549								
$C_2–(C_{14})H_3$	1.485								
$N_3–(C_4)H_3$	1.465								

[a] H–O–C angle in neutral pNph.

to the resulting transition states between M0, M1 and M0, M2 local minima, respectively (Fig. 2).

Vertical electronic excitation energy calculations were carried out using several computational methods. Excitation energies were obtained by means of the TD-DFT method with the BOP functional [37–39] and long-range corrections (LC) [22], as implemented in the quantum chemistry package *GAMESS* [40,41]. The correlation-consistent double-zeta Dunning basis set (cc-pVDZ, [42]) was used during these calculations. To evaluate solvation effects, two sets of calculations were performed. The first set corresponds to the standard gas-phase treatment of the system. For the second set, properties of the acetonitrile solvent were included using conductor-based polarizable continuum model (C-PCM) [43–45] with the following parameters: solvent radius $r_{solv} = 2.155$ Å, dielectric constants $\varepsilon = 36.64$ and $\varepsilon_{inf} = 1.806$. Additionally, the semi-empirical ZINDO approach (implemented in *Gaussian03*) and the GMC–QDPT method with cc-pVDZ basis set (found in *GAMESS*) were used to calculate excitation properties for the structures under consideration. For the GMC–QDPT calculations active space contained 5 occupied and 4 virtual orbitals; additional 28 occupied and 224 virtual orbitals were used for perturbation.

Potential energy surfaces (PES) of ground and excited electronic states of the IB compound were constructed by performing the LC-TDDFT/BOP calculations with solvent account for various structures corresponding to the different points in the reaction-coordinate phase space near the locations of the energy minima. To better evaluate the PES of the excited states of the IB compound, several excited-state optimizations were carried out. Optimizations were performed with *GAMESS* package, using the analytical TD-DFT gradient [23] with BOP functional and LC corrections, including the solvent effects. Three energy minima on the surfaces of excited electronic states were found. Energy minimum of the second excited state (S_2) is denoted E2. Its structure nearly coincides with the optimized M0 structure of the ground electronic state. Two additional energy minima of the first excited state (S_1) were also located. They are referred to as E1a and E1b further on. Positions of the optimized structures of the IB compound, as well as the shape of the ground-state PES, are presented in Fig. 2.

3. Results and discussion

3.1. Molecular structures in the ground electronic state

Structural parameters (bond lengths and bond angles) of the IB compound and its molecular groups, calculated using the DFT B3LYP functional and 6-311++(2d,p) basis set, are presented in Tables 1a and 1b. The solvent model was not used for the ground-state optimizations. General structure of the compound and numbering of atoms used throughout the discussion are shown in Fig. 1. The dashed box in Fig. 1 includes atoms corresponding to 4-nitrophenol (pNph) molecular group. A separate molecule is obtained by substituting C_2 and C_4 atoms with protons. Structure missing proton in the position of the C_2 atom represents negative 4-nitrophenol ion ($pNphe^-$). The rest of atoms shown in Fig. 1 belong to the 3H-indolium (Ind) molecular group. By omitting O_1 atom and substituting C_{29} atom with proton, chemical structure of the positive 3H-indolium ion (Ind^+) is obtained.

Table 1a holds data for neutral pNph and ionized $pNphe^-$ structures, as well as parameters of the Ind^+ structure. Optimized structures of the pNph molecule are planar. By comparing neutral and ionized forms it is clear that molecule preserves its principal structure after deprotonation. However, redistribution of the charge density results in changes up to 0.05–0.1 Å for bond lengths and up to 5° for valence angles. The Ind^+ molecule exhibits Cs symmetry, with all non-hydrogen atoms except for C_{15} and C_{16} (which correspond to the methyl groups) lying in the principal plane, while C_{15} and C_{16} are symmetrically placed on either side of the plane.

Geometric parameters of the IB compound corresponding to the structure M0 (global minimum of the potential energy surface of the ground electronic state) are shown in the first column of Table 1b. Values for the pNph part are very similar to ones of a separate neutral form (Table 1a), with main differences (less than 0.01 Å and 1°) occurring at the joining site. Values for the Ind part are, however, quite different from the Ind^+ structure. This is not surprising. If the pNph group of IB is charge-neutral in the ground state of the compound (which follows from the structure comparison), the Ind group within the compound is neutral as well, unlike the separate structure, which carries positive charge. Moreover, the biggest differences of parameters (up to 0.15 Å and 9°) again reflect changes of the links between the two groups. Combining the groups together also breaks the symmetry of the Ind molecule: C_2 and C_4 atoms are forced out of the principal plane, while methyl groups C_{15} and C_{16} are pushed away from pNph. Thus the presence of the pNph group has significant impact on the structure of the Ind group. In addition to the distinct molecular groups of pNph and Ind, the structure of the IB compound also features an oxazine ring (Fig. 1) which is created by joining the groups together. However, since the molecular groups are positioned at almost the right angle to each other, the resulting ring is deformed.

Table 1b
Parameters of the structures of the IB compound corresponding to the ground-state and excited-state energy minima. *Columns:* IB (Mx) – ground-state minima, IB (Ex) – excited-state minima.

Bond lengths (Å)							
Bond	IB (M0)	IB (M1)	IB (M2)	IB (M3)	IB (E2)	IB (E1a)	IB (E1b)
C_{13}–C_{12}	1.397	1.398	1.393	1.394	1.400	1.398	1.397
C_{12}–C_{11}	1.390	1.399	1.393	1.394	1.392	1.393	1.394
C_{11}–C_{10}	1.399	1.399	1.394	1.396	1.401	1.403	1.400
C_{10}–C_8	1.382	1.389	1.384	1.384	1.383	1.382	1.385
C_8–C_7	1.397	1.395	1.388	1.389	1.398	1.403	1.397
C_7–C_{13}	1.389	1.389	1.383	1.384	1.388	1.393	1.390
C_8–C_9	1.521	1.515	1.510	1.512	1.518	1.519	1.519
C_9–C_2	1.569	1.518	1.515	1.521	1.553	1.517	1.526
C_2–N_3	1.450	1.312	1.300	1.302	1.431	1.377	1.400
C_7–N_3	1.412	1.433	1.433	1.437	1.414	1.395	1.402
C_9–$(C_{16})H_3$	1.545	1.545	1.541	1.545	1.537	1.539	1.536
C_9–$(C_{15})H_3$	1.532	1.554	1.553	1.547	1.525	1.536	1.536
C_2–$(C_{14})H_3$	1.520	1.482	1.481	1.484	1.512	1.479	1.492
N_3–$(C_4)H_3$	1.456	1.492	1.494	1.495	1.450	1.444	1.451
C_2–O_1	1.479	*2.815*[a]	*3.209*[a]	*4.984*[a]	1.509	*2.780*[a]	*3.189*[a]
C_4–C_{29}	1.511	1.502	1.499	1.499	1.504	1.502	1.499
C_{34}–O_1	1.351	1.270	1.262	1.258	1.317	1.267	1.254
C_{34}–C_{33}	1.401	1.443	1.441	1.444	1.433	1.444	1.450
C_{33}–C_{32}	1.380	1.374	1.370	1.367	1.359	1.366	1.362
C_{32}–C_{31}	1.393	1.411	1.407	1.410	1.438	1.410	1.415
C_{31}–C_{30}	1.388	1.397	1.396	1.393	1.428	1.389	1.375
C_{30}–C_{29}	1.387	1.385	1.377	1.378	1.370	1.390	1.397
C_{29}–C_{34}	1.405	1.454	1.450	1.456	1.438	1.442	1.452
C_{31}–N_{38}	1.463	1.438	1.433	1.430	1.403	1.459	1.475
N_{38}–O_{39}	1.229	1.243	1.240	1.243	1.269	1.226	1.218
N_{38}–O_{40}	1.228	1.239	1.237	1.236	1.268	1.225	1.219
Valence angles (deg)							
Angle	IB (M0)	IB (M1)	IB (M2)	IB (M3)	IB (E2)	IB (E1a)	IB (E1b)
C_{13}–C_{12}–C_{11}	121.16	121.17	121.12	121.43	121.28	121.24	121.16
C_{11}–C_{10}–C_8	119.33	118.53	118.53	118.26	119.02	119.22	119.32
C_8–C_7–C_{13}	121.13	123.06	122.79	123.89	121.55	121.95	121.59
C_{10}–C_8–C_9	130.59	131.59	131.41	131.65	130.88	130.89	130.32
C_{13}–C_7–N_3	128.95	128.64	128.95	127.92	128.87	129.02	128.73
C_9–C_2–N_3	103.78	110.86	111.06	111.04	104.59	109.36	109.02
C_8–C_9–$(C_{16})H_3$	108.72	112.35	112.94	112.03	108.76	110.54	110.61
C_8–C_9–$(C_{15})H_3$	114.09	112.06	111.09	112.14	114.47	111.98	111.67
C_9–C_2–$(C_{14})H_3$	116.63	124.67	124.27	123.29	117.39	125.61	121.49
C_7–N_3–$(C_4)H_3$	121.06	122.52	122.85	121.68	120.72	122.38	122.96
C_9–C_2–O_1	105.95	–[b]	–[b]	–[b]	105.09	–[b]	–[b]
N_3–$(C_4)H_2$–C_{29}	111.16	110.29	113.35	112.19	110.57	110.54	108.80
C_2–O_1–C_{34}	118.46	–[b]	–[b]	–[b]	119.43	–[b]	–[b]
O_1–C_{34}–C_{33}	116.54	122.76	123.86	123.02	116.17	121.26	121.30
C_{29}–C_{34}–C_{33}	120.35	115.50	115.36	115.13	120.73	118.46	117.96
C_{33}–C_{32}–C_{31}	119.00	120.02	120.41	120.26	118.93	118.68	118.36
C_{31}–C_{30}–C_{29}	120.19	120.15	120.13	120.77	119.84	118.87	119.02
C_{32}–C_{31}–N_{38}	119.50	120.22	120.40	120.77	119.45	118.25	118.14
C_{31}–N_{38}–O_{40}	117.83	118.35	118.50	118.60	118.24	117.99	117.52
O_{39}–N_{38}–O_{40}	124.24	123.27	122.97	122.84	124.11	124.24	124.68

[a] Numbers in *italic* represent distances between C and O atoms which do not form a bond.
[b] C_2–O_1 bond is broken here.

Next three columns of Table 1b represent structures corresponding to the local minima (M1, M2, M3) in the ground electronic state energy surface of the IB compound in various phases of oxazine ring opening. Clear differentiation of two distinct groups, pNph and Ind, is observed in all cases. Values of bond lengths and angles change only slightly between the structures. Parameters of the pNph fragment closely resemble the structure of the ionized $pNphe^-$ molecule. However, there is consistent change of bond lengths by the order of 0.015–0.02 Å along the C_4–C_{29}–C_{30}–C_{31}–O_{38}–N_{40} chain. The indoline part of the structures is more or less the same as that of the separate Ind^+ ion. The differences of bond lengths and valence angles are around 0.005 Å and 0.5°, respectively.

Several geometric parameters that represent the original site of the oxazine ring for all calculated structures are gathered in Table 2. Dihedral angles $d(C_8$–C_7–N_3–$C_4)$ (out-of-plane deformation of C_4 methyl group) and $d(N_3$–C_4–C_{29}–$C_{34})$ (rotation around C_4–C_{29} bond) change consistently among all structures. However, bond angle $a(C_4$–C_{29}–$C_{34})$ (tilt of pNph group into Ind group) does not vary significantly. Thus the reaction path in the ground state potential energy surface of the IB compound can qualitatively be described by rotation of the pNph group around the C_4–C_{29} bond and the subsequent symmetrization of the indolium group, without bending the pNph group away from Ind. Following this finding dihedral angles $d(C_8$–C_7–N_3–$C_4)$ and $d(N_3$–C_4–C_{29}–$C_{34})$ are used here as the principal coordinates for the potential energy surfaces (PES) of the IB compound. The C_2–O_1 bond of the initial oxazine ring is broken by rotating the pNph group. The distance between C_2 and O_1 atoms and corresponding values of the relative ground-state energy for various structures are depicted in Fig. 3. The calculated distance of 1.479 Å for the optimal M0 structure coincides with the value that follows from the X-ray crystallographic data [5].

Table 2
Structural parameters of the IB compound representing the original site of the oxazine ring at various points of the ground-state PES. Most relevant parameters (proposed reaction coordinates) are **bold**. The distance r given in angstroms, valence angles a and dihedrals d – in degrees.

	M1	E1a	T01	M0	E2	T02	M2	E1b	M3
$r(O_1–C_2)$	*2.943*	*2.780*	*2.436*	1.479	1.509	*2.524*	*3.209*	*3.189*	*4.984*
$d(C_8–C_7–N_3–C_4)$	**172.062**	**172.469**	**161.884**	**155.413**	**154.682**	**165.571**	**175.134**	**153.875**	**177.362**
$a(N_3–C_4–C_{29})$	111.626	110.544	108.646	111.163	110.567	116.041	113.351	108.797	112.191
$d(N_3–C_4–C_{29}–C_{34})$	**−61.139**	**−55.837**	**−50.091**	**−17.068**	**−20.186**	**33.520**	**49.197**	**54.089**	**108.138**
$a(C_4–C_{29}–C_{34})$	117.829	117.320	118.470	118.963	117.808	120.565	116.869	118.269	117.193

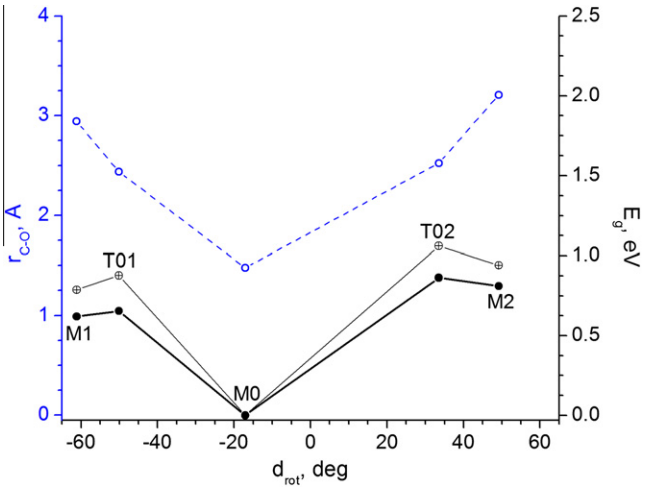

Fig. 3. Dependence of bond $C_2–O_1$ length (dashed line) and relative ground-state energy (solid lines) on rotation angle $N_3–C_4–C_{29}–C_{34}$ between the two molecular groups of the IB compound. Positions of calculated structures are marked by black circles (based on DFT B3LYP calculations using 6-311++(2d,p) basis set) and crossed circles (based on DFT BOP/LC calculations using cc-pVDZ basis set and the solvent model).

3.2. Molecular structures in the excited electronic states

Geometry parameters of the structures of the IB compound corresponding to the local minima of the excited electronic states (blue labels in Fig. 2) are shown in the last three columns of Table 1b. Comparing the structure of the excited-state minimum E2 (fifth column) with the global minimum structure M0 (first column) reveals almost no change in the indolium group (with the only exception being the carbon atom of the $C_2–O_1$ bond). However, parameters of the pNph group differ by as much as 0.06 Å between the structures. This suggests that the excitation of the IB compound in ground state primarily affects the nitrophenol part of the compound before the ring opening takes place. Another comparison can be done near the local ground-state energy minimum M1 (second column), where excited-state minimum E1a is found (sixth column). The central fused-ring part of the Ind group is again almost unchanged, while differences by the order of 0.02–0.04 Å are observed for the methylated part. Parameters of the pNph group are also very similar between the M1 and E1a structures, except for the NO_2 part (changes of 0.01–0.02 Å). Thus the excitation at the site of the local energy minimum involves different parts of the IB compound – methyl groups of Ind and the NO_2 group of pNph are affected instead of the entire pNph moiety. Finally, the comparison of structural parameters at the local ground-state energy minimum M2 (third column) and the minimum of the first excited state E1b (seventh column) yields more significant differences between the structures; these points are not as close to each other in the space of the proposed reaction coordinates (Table 2, Fig. 2) as the first two pairs. Nevertheless, the central part of the Ind group is observed to be quite rigid – it retains its form even between distant PES points.

3.3. Potential energy surface in the ground electronic state

The ground-state potential energy values for the structures of the IB compound relative to the energy of the global minimum structure M0 are pictured in Fig. 3. Energy values denoted by black circles are based on the results of the original DFT optimizations using the B3LYP functional and 6-311++(2d,p) basis set. Crossed circles correspond to the values obtained using the BOP functional with cc-pVDZ basis set, LC corrections and C-PCM solvent model for acetonitrile. It is clear that while the use of the BOP functional results in slightly different estimation of the energy values, it does not bring qualitative changes. The local minima M1 and M2 correspond to similar structures with respect to the parameters characterizing oxazine ring opening. The distances between C_2 and O_1 atoms are 2.94 and 3.21 Å, and the relative potential energy of resulting structures is respectively 0.62 and 0.81 eV higher than the energy of the M0 structure. The small difference between ground-state energies of the M1 and M2 structures is also supported by the results of other methods. Structures of T01 and T02 correspond to the transition states between the initial structure M0 and open-ring structures M1 and M2, respectively. Energy values for states T01 and T02 are 0.654 and 0.862 eV with respect to the M0 structure. Comparable values of 17.6 kcal/mol (0.763 eV) for the open-ring state and 18.1 kcal/mol (0.785 eV) for the transition state were already reported [5] (calculated using the DFT B3LYP functional and 6-31G(d) basis set). Energy barriers for transitions from M1 and M2 structures to the M0 structure are equal to 0.035 and 0.052 eV (1.4 and 2.0 k_BT), respectively. Small energy barriers indicate that open-ring system can convert to the M0 structure in the ground electronic state due to thermal influence. The overall shape of the ground-state potential energy surface in the space of dihedral angles $d(C_8–C_7–N_3–C_4)$ and $d(N_3–C_4–C_{29}–C_{34})$ (Table 2) can be seen in Fig. 2. It contains a clearly distinguishable area of lower energy around the global minimum structure M0, while the rest of the surface is relatively flat and the local minima are shallow. The shape of the PES suggests that the behavior of the excited system after returning to the ground state is not rigidly constrained and that some variation in the resulting structures – leading to the variation of the observed spectral properties – is expected for some time after the initial excitation.

3.4. Excited-state energies and the wavefunction character

Vertical electronic excitation energies of the IB compound and its molecular groups are given in Tables 3a and 3b (calculated by means of the TD-DFT method), Table 3c (calculated using the ZINDO approach) and Table 3d (calculated by the GMC–QDPT method). For comparison, peaks experimentally defined by using the steady-state absorption and pump-probe measurements [6] are referred to throughout the discussion and shown in Fig. 4 next to theoretical values. Ground state of a molecular compound or its conformation is denoted S_0 further on, while labels S_1, S_2 etc. are used to mark singlet excited states in the order of increasing excitation energy. When referring to the wavefunction data we use number 1 for highest occupied molecular orbital (HOMO), 2 for

Table 3a
Excitation energies of the molecular groups of the IB compound calculated using TD-DFT/BOP with the LC corrections, cc-pVDZ basis set, and the C-PCM solvent model. **Bold** numbers indicate transition-allowed excitations (with calculated oscillator strength > 0.1). Energy values given in eV.

Exc.	No solvent			Solvent – acetonitrile (C-PCM)		
	pNph	$pNphe^-$	Ind^+	pNph	$pNphe^-$	Ind^+
1	3.925	**3.895**	**4.709**	4.037	**3.726**	**4.896**
2	4.458	3.897	5.083	4.551	3.931	5.224
3	**5.072**	4.219	5.976	**4.719**	4.330	**6.092**
4	5.133	4.598	6.538	5.044	4.673	**6.527**
5	6.223	4.683	**6.554**	5.981	4.709	6.691
6	6.744	5.429	6.806	6.735	5.444	6.912
7	6.864	5.595	7.125	6.745	5.659	7.129
8	7.390	6.531	7.410	7.194	6.476	7.340

HOMO−1, 3 for HOMO−2 and so on. Lowest unoccupied orbital (LUMO) is denoted by 1′, LUMO + 1 by 2′ etc.

One strongly optically allowed transition is expected in both neutral (pNph) and ionized ($pNphe^-$) forms of the 4-nitrophenol fragment. Upon deprotonation, it shifts to the red side of the spectrum. According to the TD-DFT calculations without solvent account, the energy values of the lowest excitation are 5.07 eV for the neutral form and 3.90 eV for the ionized form of pNph (Table 3a). This constitutes a redshift of 1.17 eV. Use of the solvent model results in lower excitation energy values – 4.72 eV and 3.73 eV for pNph and $pNphe^-$, respectively – and the redshift of 0.99 eV. Similar result is obtained using the ZINDO approach (from 3.84 to 2.81 eV, Table 3c) and is in accord to the experimental data (from 4.01 to 2.99 eV) [6], although it is evident that the TD-DFT method overestimates the absolute value of the excitation energy. Excitation of the pNph molecule mainly corresponds to 1–1′ (HOMO–LUMO) electron transfer (Fig. 5, left and center), so the shift of the absorption band is most likely to be caused by changes in the energy gap between HOMO and LUMO, when these orbitals are slightly modified as a result of the proton detachment. The absorption spectrum of Ind^+ also consists of one low-lying excitation. Computed energy value of this excitation is 4.71 eV and 4.90 eV using the TD-DFT calculations in gas phase and with solvent model, respectively. The results agree fairly well with those obtained using the GMC–QDPT method and the experimental data (4.61 and 4.46 eV), while the ZINDO approach heavily underestimates the value of the excitation energy (3.83 eV). The most significant contribution to the excitation comes from 2 to 1′ electron transfer (Fig. 5, right), during which internal charge is redistributed from the benzene ring towards the indoline heterocycle and its methyl groups.

The lowest optically allowed excitation of the IB compound (at the global minimum structure M0) is within the same spectral region as the one in the pNph group, with the reported experimental value of 4.11 eV (300 nm [6]). Theoretical values obtained using the TD-DFT method equal to 4.84 eV (gas phase) and 4.56 eV (solvent model for acetonitrile). The GMC–QDPT calculations give give the value of 4.30 eV, while using the ZINDO approach results in the lower excitation energy of 3.66 eV. The energy values are quite close to the excitation energy of the neutral pNph molecule for the respective methods, and both overestimation of the energy values by TD-DFT and underestimation by ZINDO are consistent

Table 3b
Excitation energies of the IB compound calculated using TD-DFT/BOP with the LC corrections, cc-pVDZ basis set, and the C-PCM solvent model.

Exc.	No solvent				Solvent – acetonitrile (C-PCM)						
	IB (M0)	IB (T01)	IB (M1)	IB (M2)	IB (M0)	IB (E2)	IB (T01)	IB (M1)	IB (E1a)	IB (M2)	IB (E1b)
1	3.907	2.589	2.912	2.668	4.007	3.619	**3.612**	**3.687**	2.992	**3.728**	2.041
2	4.447	**3.670**	3.404	3.313	4.527	**3.799**	3.995	4.043	3.465	**3.842**	2.893
3	**4.840**	3.921	3.924	3.929	**4.560**	4.193	4.054	**4.090**	**3.836**	4.051	**3.760**
4	4.989	4.463	**4.218**	**4.145**	4.903	4.655	**4.314**	4.353	4.221	4.395	**3.801**
5	5.009	**4.644**	4.539	4.473	4.969	4.708	4.656	4.649	4.417	4.545	4.322
6	5.358	4.824	4.557	4.572	5.106	4.982	4.738	4.670	4.516	4.558	4.352
7	5.682	4.929	4.811	4.682	5.618	5.451	4.753	4.681	4.710	4.692	4.403
8	5.956	5.076	4.977	4.952	5.812	5.596	5.177	5.019	4.723	4.966	4.535

Table 3c
Excitation energies of the IB compound and its molecular groups calculated using the ZINDO approach.

Exc.	pNph	$pNphe^-$	Ind^+	IB (M0)	IB (T01)	IB (M1)	IB (M2)	IB (M3)
1	2.539	2.674	**3.831**	2.533	2.569	2.365	2.135	2.180
2	2.755	**2.813**	4.298	2.760	**2.843**	2.601	2.608	2.615
3	**3.843**	3.086	4.739	**3.660**	2.859	**2.904**	**2.847**	**2.809**
4	4.202	3.187	5.219	4.009	3.075	2.912	2.922	2.953
5	5.005	3.975	5.969	4.156	3.730	3.254	3.254	3.378
6	5.340	4.293	5.996	4.319	3.924	3.600	3.498	3.764
7	5.351	4.707	6.184	4.724	4.033	3.867	3.816	3.818
8	6.164	5.081	6.193	4.839	4.402	4.153	4.015	3.948

Table 3d
Excitation energies of the IB compound and its molecular groups calculated using the GMC–QDPT method with cc-pVDZ basis set.

Exc.	pNph	$pNphe^-$	Ind^+	IB (M0)	IB (T01)	IB (M1)	IB (M2)	IB (M3)
1	4.214	**3.256**	4.080	3.756	**2.606**	**2.407**	2.219	2.173
2	**4.916**	3.849	**4.609**	3.865	**3.682**	**3.726**	**3.613**	**3.503**
3	5.716	4.895	5.107	**4.298**	4.474	4.374	**4.283**	4.230
4	5.997	5.134	6.163	4.566	**4.579**	4.513	4.367	4.301
5	6.427	5.654	6.540	4.740	4.877	**5.045**	**4.986**	**4.823**

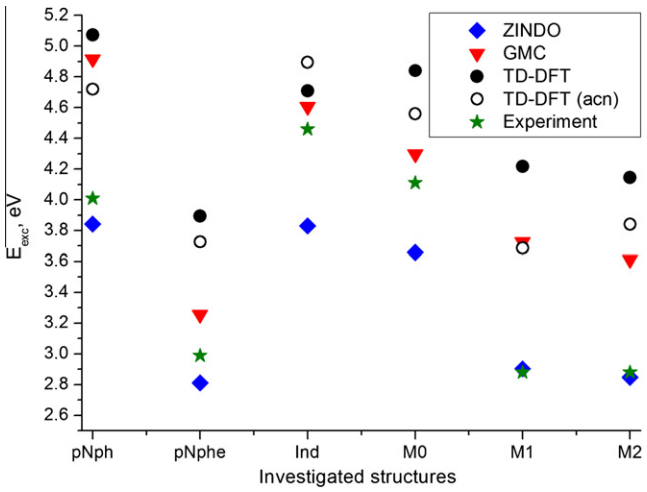

Fig. 4. Excitation energies of stable structures of the IB compound in the ground electronic state and of its chromophoric groups.

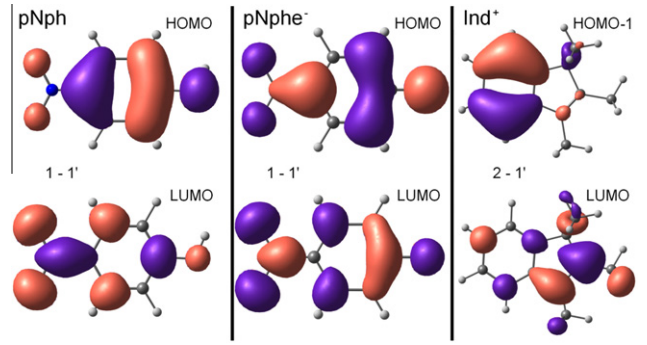

Fig. 5. Molecular orbitals of the lowest optically allowed excitation in 4-nitrophenol and 3H-indolium (based on TD-DFT calculations). Numbers 1, 2, 3,... denote occupied orbitals (starting from HOMO), 1′, 2′, 3′,... – unoccupied orbitals (starting from LUMO).

with the results for the separate moieties. Most significant electronic transfer for this excitation is 2–1′. Results of TD-DFT (Fig. 6) and GMC-QDPT (Fig. 7) calculations match in both the position and the shape of the respective molecular orbitals. The lowest unoccupied molecular orbital 1′ is almost identical to LUMO of the separate 4-nitrophenol molecule, while orbital 2 corresponds to HOMO of the same molecule. Therefore it can be concluded that the initial excitation of the IB compound acts mainly on the pNph group of the compound. The structure M0 also exhibits initial charge separation of 0.18 *e* between the molecular groups. Calculated excitation energies for the structures with open oxazine ring (M1 and M2 in Fig. 4) are significantly lower and similar to that of the ionized pNphe$^-$ group. Properties of these structures are discussed in more detail later on.

It is clear from Fig. 4 that all theoretical methods used here describe absorption of the IB compound in a way that is qualitatively consistent with experimental data. However, the energy values differ by a few tenths of electronvolt. The TD-DFT and GMC–QDPT methods tend to overestimate energy values, while using the semi-empirical ZINDO approach results in lower excitation energies. These differences may arise from the practical constraints of the methods used for calculations, such as limited active space for reference configurations (chosen on the grounds of computational costs) in GMC–QDPT. Addition of solvent effects gives closer estimation of excitation energies in most cases.

3.5. Potential energy surfaces in the excited electronic states

Relative energy values of the points on the potential energy surfaces of low-lying optically allowed excited states with respect to the ground-state energy of the M0 structure were estimated in the following way:

$$E_{pot}(i) = E(S_0) + E_{exc}(i) \quad (1)$$

where $E(S_0)$ is the relative ground-state energy of the structure under consideration, and $E_{exc}(i)$ is the excitation energy from the ground to the *i*th state. Results for various computational methods are summarized in Tables 4a and 4b. Molecular orbitals of the relevant electronic states for various structures are presented in Fig. 6 (based on TD-DFT calculations) and in Fig. 7 (based on GMC–QDPT calculations).

Potential energy surfaces of the excited states further from the global minimum structure M0 are relatively flat – decrease of the excitation energy at the local minima and transition states is compensated by the rise of the relative ground-state energy (compare third and fourth columns of Tables 4a and 4b). However, several remarks can be made about the obtained results. First, the optical transition from the ground-state structure M0 occurs mainly to the state S_3. The lowest optically-allowed excitation calculated for every other structure corresponds to the transition to the

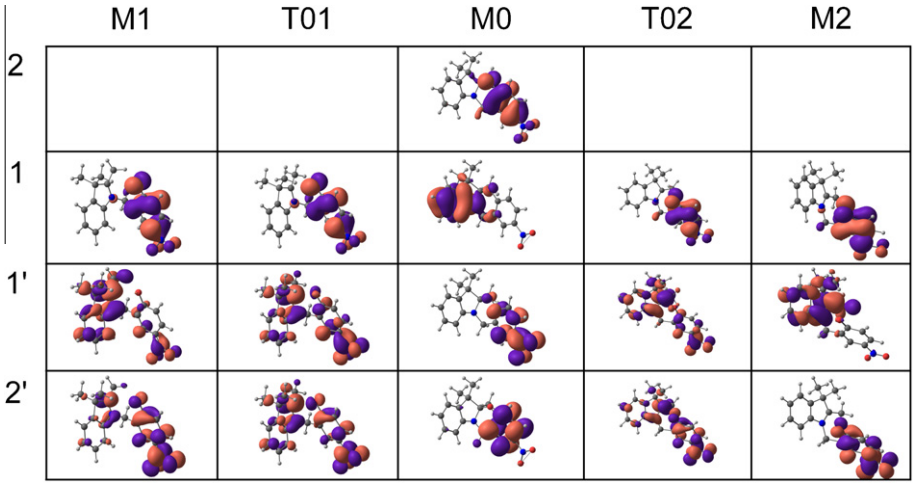

Fig. 6. Molecular orbitals of the IB compound at various points of the ground-state potential energy surface (based on TD-DFT calculations).

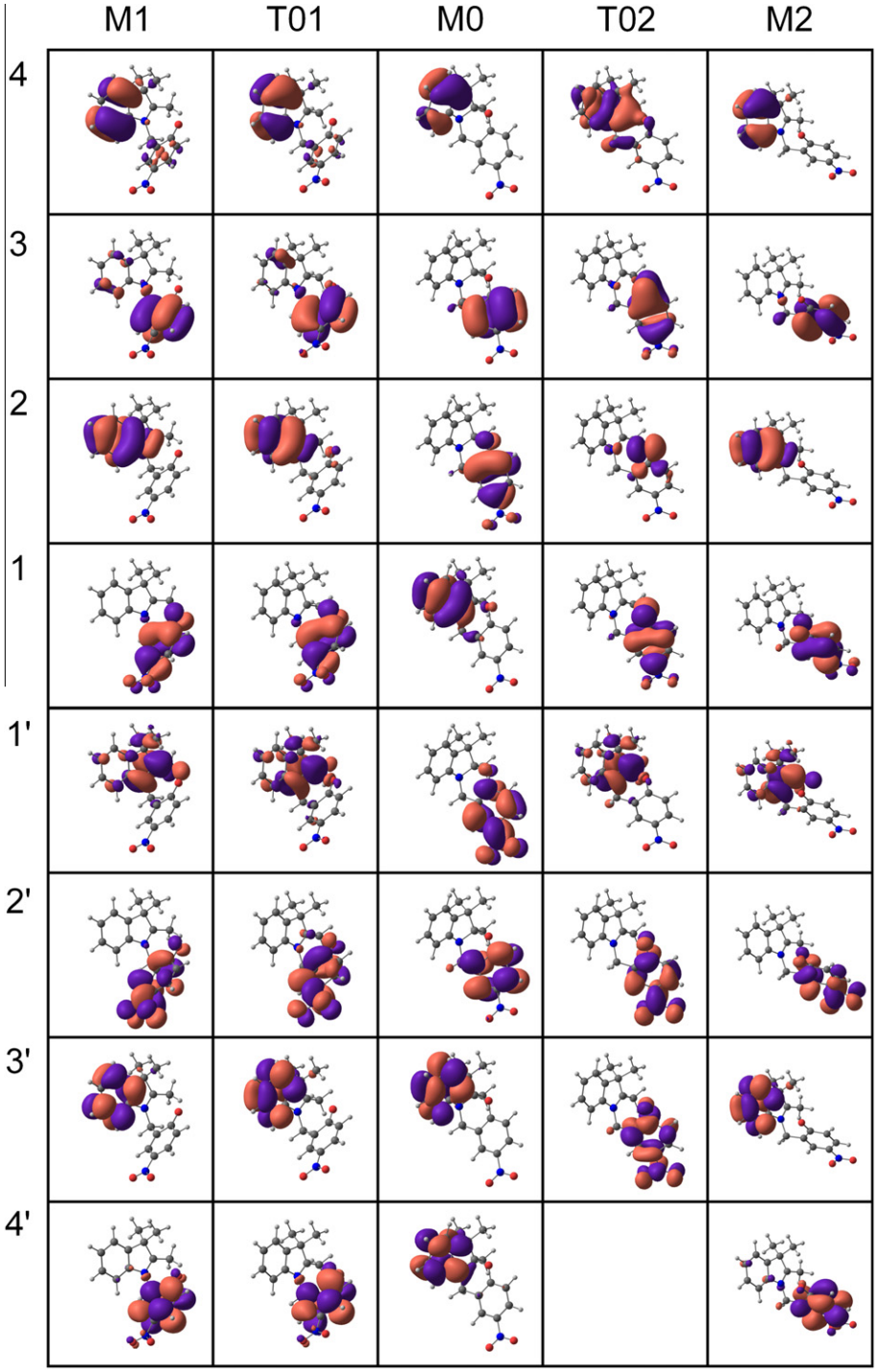

Fig. 7. Molecular orbitals of the IB compound at various points of the ground-state potential energy surface (based on GMC–QDPT calculations).

excited state S_1 (S_2 in the case of M2). This indicates the possibility of the state-crossing or state-mixing at some point during the excitation process. Second, results for the structures obtained by rotating pNph group in one direction (T01 and M1) are not symmetric to the results for the structures situated in the opposite side (T02 and M2). It follows from the TD-DFT calculations that the potential energy of the lowest excited state for structures T01 and M1 is slightly lower than the corresponding energy for the M0 structure, while the energies for structures T02 and M2 are somewhat higher. In the GMC–QDPT case the lowest excited state of the compound calculated at the M2 structure becomes optically forbidden. Since neither pathway of the structural deformation of the IB compound seems to be highly energetically favorable (Fig. 3), both of them may be active at the same time during the excitation process. The differences of the other properties would then result in more complicated spectra.

Wavefunction character of optically-allowed low-lying excitation of the initial M0 structure is similar to the corresponding excitation of separate pNph molecule. It is mainly attributed to an electron transfer between 2 and 1′ molecular orbitals (Fig. 6) and involves mostly pNph group. Breaking the C_2–O_1 bond introduces significant changes to the shape and ordering of molecular orbitals

Table 4a
Parameters of low-lying active excited states of the IB compound at various points of the ground-state PES (based on TD-DFT/BOP calculations with cc-pVDZ basis set and C-PCM solvent model). E_{exc} – excitation energy, E_{pot} – potential energy relative to the energy of the M0 structure, f – oscillator strength. Numbers 1, 2, 3,... denote occupied orbitals (starting from HOMO), 1′, 2′, 3′,... – unoccupied orbitals (starting from LUMO).

Structure	State no.	E_{exc}, eV	E_{pot}, eV	f	MOs	Weight
M1	S_1	3.687	4.473	0.391	1–1′	0.886
	S_3	4.089	4.875	0.173	1–2′	0.853
T01	S_1	3.612	4.488	0.459	1–1′	0.946
	S_4	4.314	5.191	0.180	1–2′	0.704
M0	S_3	4.560	4.560	0.466	2–1′	0.936
T02	S_1	3.606	4.666	0.530	1–1′	0.935
M2	S_1	3.728	4.668	0.162	1–1′	0.900
	S_2	3.842	4.782	0.432	1–2′	0.889

Table 4b
Parameters of low-lying active excited states of the IB compound at various points of the ground-state PES (based on GMC–QDPT calculations).

Structure	State no.	E_{exc}, eV	E_{pot}, eV	f	MOs	Weight
M1	S_1	2.407	3.027	0.155	1–1′	0.618
	S_2	3.726	4.346	0.313	1–3′	0.620
	S_5	5.045	5.665	0.311	3–1′	0.594
T01	S_1	2.606	3.260	0.302	1–1′	0.613
	S_2	3.682	4.336	0.156	1–2′	0.592
	S_4	4.579	5.233	0.253	3–1′	0.520
M0	S_3	4.298	4.298	0.167	2–1′	0.475
T02	S_1	2.588	3.450	0.262	1–4′	0.556
	S_2	3.284	4.146	0.131	3–4′	0.484
	S_3	3.850	4.712	0.397	1–6′	0.517
M2	S_1[a]	*2.219*	*3.029*	*0.020*	*1–1′*	*0.615*
	S_2	3.613	4.423	0.440	1–3′	0.615
	S_3	4.283	5.093	0.159	5–1′	0.449
	S_5	4.986	5.796	0.251	3–1′	0.585
M3	S_1[a]	*2.173*	*2.967*	*0.077*	*1–1′*	*0.614*
	S_2	3.503	4.297	0.386	1–3′	0.616
	S_5	4.823	5.617	0.321	4–1′	0.488

[a] S_1 state for structures M2 and M3 has negligible oscillator strength, but is provided for comparison with M1 structure.

of the compound. From the TD-DFT calculations it follows that the lowest-lying dipole allowed excitation mainly corresponds to the 1–1′ electron transfer for all open-ring structures. The ground-state wavefunction of the optically allowed excitations for the structures T01, M1, T02 and M2 is similar to the corresponding wavefunction of the transition at the initial M0 structure and belongs mostly to the pNph group. On the other hand, the excited-state wavefunction is also partially (and sometimes fully) distributed over Ind fragment in these cases (Fig. 6). This suggests that during deexcitation (e.g. from the excited-state minimum E1a with molecular structure similar to M1) electron density is likely to redistribute from Ind group towards the joining point and to the pNph group, which facilitates charge separation between the two molecular groups. The partial charge of the pNph group at the local minima and transition structures does not change much and equals to about 0.5 *e* (increase of 0.32 *e* from the initial M0 structure). This suggests that the opening of the oxazine ring has immediate impact on the electronic part of the system, although the charge redistribution is fairly modest.

Description of the excited-state potential energy surfaces of the IB compound can be improved by performing optimizations of certain excited states and analyzing behavior of the system. Two out of three local excited-state energy minima that were found during the optimizations, E2 and E1a, are close to the ground-state minima (M0 and M1, respectively). Presence of the local minimum E1a provides the means for the IB compound to reach the ground-state energy minimum (M1) after the photoexcitation and form a relatively stable reaction product. The local minimum structure E2 is close to the initial structure M0 without coinciding with it. The main excitation of the initial structure transfers system into the state S_3. However, energy of this state is almost identical to the energy of S_2 at the same point (Table 3b). Therefore, the state-crossing or non-optical conversion is possible, followed by the steep descent to the adjacent minimum point. The potential energy of the lowest-lying optically-allowed excited state at the M0 and E2 structures is 4.560 eV and 3.799 eV, respectively, resulting in a difference of 0.76 eV (Table 3b). Decrease of the potential energy can be converted into the kinetic energy of the system during this process and eventually lead to the opening of the oxazine ring.

Relatively high oscillator strength for excitations to more than one low-lying excited state for all open-ring structures determines the main difference of results obtained by using GMC–QDPT from ones achieved by other methods. These states can be split into three groups with different excitation energies that should in principle be distinguishable in the experiment. Most intensive excitation with the energy of 3.5–3.7 eV corresponds to the electron transfer 1–3′ between the benzene ring of the Ind group and the HOMO of the pNph group (Fig. 7). The nature of changes in the wavefunction during this excitation is similar to the one obtained by the TD-DFT method. The second group of states is described by electron transfer between LUMO of the Ind group and the central ring part of pNph (3–1′ for the M1 structure). The energy of this excitation is higher and equal to about 4.8–5.0 eV. Finally, the excitation at local minimum M1 (but not M2) is mainly described by the 1–1′ (HOMO–LUMO) electron transfer with corresponding excitation energy of 2.2–2.4 eV. Analysis of changes in the wavefunction character upon excitation of local minima structures shows that the electronic charge is redistributed in the same direction (from pNph to Ind group in the case of absorption in the ground electronic state) in all cases.

4. Conclusions

Quantum chemical calculations of the IB compound and its molecular groups show that the oxazine ring is formed within the molecule in its ground electronic state. However, deformation of this ring suggests that it may be prone to the external impact, such as photoexcitation. Furthermore, during the formation of the IB compound the symmetry of its Ind group is broken. Upon cleavage of C_2–O_1 bond (Fig. 1) and subsequent rotation of the pNph group, both parts of the compound assume structures very similar to the ions of separate groups connected by a short chain of C and O atoms. Existence of this chain makes rotation of the molecular groups around the single bond preferable to bending deformation. Three local minima on the ground-state potential energy surface were found along the path of rotation. Two closest minima are separated from the global minimum structure by the transition energy barriers of less than 2 k_BT, making them likely to revert to the initial structure by thermalization.

Calculations of vertical electronic excitations of the IB compound and its parts using different computational methods show similar properties and relations between various structures. Obtained values for the excitation energies are within a few tenths of eV from the experimental data. The results of calculation of energies and wavefunction characters of excited states by different computational methods show that singly-excited configuration based methods give qualitatively similar results to the more sophisticated (and more computationally expensive) GMC–QDPT method. However, particular methods have drawbacks for specific type of structures. This shows the need of investigation of complex systems by means of several methods at once. The TD-DFT calculations tend to overestimate the excitation energies, but are overall qualitatively correct and do not seem to exhibit problems

commonly associated with the treatment of charge-transfer systems. This is likely the consequence of using the LC scheme to correct for long-range interactions and the relatively weak charge redistribution effect in the IB compound. Results obtained by GMC–QDPT are also in good agreement with the experiment. They demonstrate more complex wavefunction character for the excitations of IB compound compared to the other methods.

It may be concluded that the photoexcitation of the IB compound in its ground electronic state results in the excitation of the pNph molecular group with partial charge redistribution towards this group. Opening of the oxazine ring immediately divides the compound into two parts, properties of which resemble those of the separate molecular groups. Subsequent transformation of the molecule by the rotation around C–C bond takes place in the excited state. Energy relaxation of the transformed system further facilitates charge separation between two molecular groups, which then acquire ionic character. After relaxation molecule is likely to fall into a shallow local minimum on the PES of the ground electronic state, from where it reverts to the initial structure due to thermal influence. Deexcitation without the full transformation to an open-ring structure may also be possible.

Results achieved during the investigation of the electronic singlet ground- and excited-state potential energy surfaces for structures of the IB compound close to the global minimum structure will be a starting point for future studies of the excited-state dynamics and subsequent relaxation of the modeled compound.

Acknowledgements

This research was supported by EC structural funds projects SFMIS BPD2004-ERPF-1.5.0-12-05/0013 and BPD2004-ESF-2.5.0-03-05/0012 and by the European Social Fund under the Global Grant Measure (ST, JS and LV). The public access supercomputer from the High Performance Computing Center (HPCC) of the Lithuanian National Center of Physical and Technology Sciences (NCPTS) at Vilnius University was used.

References

[1] T. Hugel, N.B. Holland, H.E. Gaub, Science 296 (2002) 1103.
[2] M. Irie, Chem. Rev. 100 (2000) 1683.
[3] H. Dürr, H. Bouas-Laurent (Eds.), Photochromism: Molecules and Systems, Elsevier, Amsterdam, 1990.
[4] C.B. McArdle (Ed.), Applied Photochromic Polymer Systems, Blackie, Glasgow, 1992.
[5] M. Tomasulo, S. Sortino, A.J.P. White, F.M. Raymo, J. Org. Chem. 70 (2005) 8180.
[6] M. Barkauskas, V. Martynaitis, A. Šačkus, R. Rotomskis, V. Sirutkaitis, M. Vengris, Lith. J. Phys. 48 (2008) 231.
[7] A.O. Bulanov, L.D. Popov, I.N. Scherbakov, Spectroch. Acta A 71 (2008) 1146.
[8] L.L. Premvardhan, F. Buda, R.v. Grondelle, J. Phys. Chem. B 108 (2004) 5138.
[9] T. Sakata, Y. Kawashima, H. Nakano, J. Phys. Chem. A 114 (2010) 12363.
[10] D.A. Lutterman, A.A. Rachford, J.J. Rack, C. Turro, J. Phys. Chem. Lett. 1 (2010) 3371.
[11] A. Shachkus, J. Degutis, A. Jezerskaite, in: J. Kovac, P. Zalupsky (Eds.), Chem. Heterocyclic Compounds **35**, Elsevier, Amsterdam, 1988, p. 518.
[12] M. Tomasulo, S. Sortino, F.M. Raymo, J. Org. Chem. 73 (2008) 118.
[13] R. Bauernschmitt, R. Ahlrichs, Chem. Phys. Lett. 256 (1996) 454.
[14] M.E. Casida, C. Jamorski, K.C. Casida, D.R. Salahub, J. Chem. Phys. 108 (1998) 4439.
[15] R.E. Stratmann, G.E. Scuseria, M.J. Frisch, J. Chem. Phys. 109 (1998) 8218.
[16] F. Furche, R. Ahlrichs, J. Chem. Phys. 117 (2002) 7433.
[17] J.E. Ridley, M.C. Zerner, Theor. Chem. Acc. 32 (1973) 111.
[18] M.C. Zerner, in: K.B. Lipkowitz, D.B. Boyd (Eds.), Rev. Comput. Chem., vol. 2, VCH Publishing, New York, 1991, p. 313.
[19] H. Nakano, R. Uchiyama, K. Hirao, J. Comp. Chem. 23 (2002) 1166.
[20] M. Miyajima, Y. Watanabe, H. Nakano, J. Chem. Phys. 24 (2006) 044101.
[21] R. Ebisuzaki, Y. Watanabe, H. Nakano, Chem. Phys. Lett. 442 (2007) 164.
[22] Y. Tawada, T. Tsuneda, S. Yanagisawa, Y. Yanai, K. Hirao, J. Chem. Phys. 120 (2004) 8425.
[23] M. Chiba, T. Tsuneda, K. Hirao, J. Chem. Phys. 124 (2006) 144106.
[24] M.J. Frisch, G.W. Trucks, H.B. Schlegel, G.E. Scuseria, M.A. Robb, J.R. Cheeseman, J.A. Montgomery, Jr., T. Vreven, K.N. Kudin, J.C. Burant, J.M. Millam, S.S. Iyengar, J. Tomasi, V. Barone, B. Mennucci, M. Cossi, G. Scalmani, N. Rega, G.A. Petersson, H. Nakatsuji, M. Hada, M. Ehara, K. Toyota, R. Fukuda, J. Hasegawa, M. Ishida, T. Nakajima, Y. Honda, O. Kitao, H. Nakai, M. Klene, X. Li, J.E. Knox, H.P. Hratchian, J.B. Cross, V. Bakken, C. Adamo, J. Jaramillo, R. Gomperts, R.E. Stratmann, O. Yazyev, A.J. Austin, R. Cammi, C. Pomelli, J.W. Ochterski, P.Y. Ayala, K. Morokuma, G.A. Voth, P. Salvador, J.J. Dannenberg, V.G. Zakrzewski, S. Dapprich, A.D. Daniels, M.C. Strain, O. Farkas, D.K. Malick, A.D. Rabuck, K. Raghavachari, J.B. Foresman, J.V. Ortiz, Q. Cui, A.G. Baboul, S. Clifford, J. Cioslowski, B.B. Stefanov, G. Liu, A. Liashenko, P. Piskorz, I. Komaromi, R.L. Martin, D.J. Fox, T. Keith, M.A. Al-Laham, C.Y. Peng, A. Nanayakkara, M. Challacombe, P.M.W. Gill, B. Johnson, W. Chen, M.W. Wong, C. Gonzalez, J.A. Pople, Gaussian 03, Revision D.01, Gaussian, Inc., Wallingford CT, 2004.
[25] P. Hohenberg, W. Kohn, Phys. Rev. 136 (1964) B864.
[26] W. Kohn, L.J. Sham, Phys. Rev. 140 (1965) A1133.
[27] R.G. Parr, W. Yang, Density-Functional Theory of Atoms and Molecules, Oxford Univ. Press, Oxford, 1989.
[28] A.D. Becke, J. Chem. Phys. 98 (1993) 5648.
[29] C. Lee, W. Yang, R.G. Parr, Phys. Rev. B 37 (1988) 785.
[30] B. Miehlich, A. Savin, H. Stoll, H. Preuss, Chem. Phys. Lett. 157 (1989) 200.
[31] A.D. McLean, G.S. Chandler, J. Chem. Phys. 72 (1980) 5639.
[32] K. Raghavachari, J.S. Binkley, R. Seeger, J.A. Pople, J. Chem. Phys. 72 (1980) 650.
[33] M.J. Frisch, J.A. Pople, J.S. Binkley, J. Chem. Phys. 80 (1984) 3265.
[34] T. Clark, J. Chandrasekhar, G.W. Spitznagel, J. Comp. Chem. 4 (1983) 294.
[35] C. Peng, H.B. Schlegel, Israel J. Chem. 33 (1993) 449.
[36] C. Peng, P.Y. Ayala, H.B. Schlegel, M.J. Frisch, J. Comp. Chem. 17 (1996) 49.
[37] A.D. Becke, Phys. Rev. A38 (1988) 3098.
[38] T. Tsuneda, K. Hirao, Chem. Phys. Lett. 268 (1997) 510.
[39] T. Tsuneda, T. Suzumura, K. Hirao, J. Chem. Phys. 110 (1999) 10664.
[40] M.W. Schmidt, K.K. Baldridge, J.A. Boatz, S.T. Elbert, M.S. Gordon, J.H. Jensen, S. Koseki, N. Matsunaga, K.A. Nguyen, S. Su, T.L. Windus, M. Dupuis, J.A. Montgomery, J. Comp. Chem. 14 (1993) 1347.
[41] M.S. Gordon, M.W. Schmidt, in: C.E. Dykstra, G. Frenking, K.S. Kim, G.E. Scuseria (Eds.), Theory and Applications of Computational Chemistry: The First Forty Years, Elsevier, Amsterdam, 2005, p. 1167.
[42] T.H. Dunning Jr., J. Chem. Phys. 90 (1989) 1007.
[43] M. Cossi, V. Barone, J. Chem. Phys. 115 (2001) 4708.
[44] Y. Wang, H. Li, J. Chem, Phys. 131 (2009) 206101.
[45] Y. Wang, H. Li, J. Chem. Phys. 133 (2010) 034108.